Received: 5 March 2024 | Revised: 14 May 2024 | Accepted: 18 May 2024

DOI: 10.1002/cbf.4065

RESEARCH ARTICLE

CELL BIOCHEMISTRY & FUNCTION WILEY

An exploratory study on the effect of kynurenine metabolites on sEnd-2 endothelioma cells

Danielle Sandra Nkandeu[1] | Anna Margaretha Joubert[1] | June Cheptoo Serem[2] | Priyesh Bipath[1] | Yvette Nkondo Hlophe[1]

[1]Department of Physiology, School of Medicine, Faculty of Health Sciences, University of Pretoria, Pretoria, South Africa

[2]Department of Anatomy, School of Medicine, Faculty of Health Sciences, University of Pretoria, Pretoria, South Africa

Correspondence
Yvette Nkondo Hlophe, Department of Physiology, School of Medicine, Faculty of Health Sciences, University of Pretoria, Private Bag X323, Gezina, Pretoria, Gauteng 0031, South Africa.
Email: Yvette.hlophe@up.ac.za

Funding information
The National Research Foundation (NRF), Grant/Award Numbers: A1F4685, N1F580; The University Capacity Development Programme (UCDP), Grant/Award Numbers: A1D783, N1F120

Abstract

Cancer is the second leading cause of mortality worldwide. The development of anticancer therapy plays a crucial role in mitigating tumour progression and metastasis. Epithelioid hemangioendothelioma is a very rare cancer, however, with a high systemic involvement. Kynurenine metabolites which include L-kynurenine, 3-hydroxykynurenine, 3-hydroxyanthranilic acid and quinolinic acid have been shown to inhibit T-cell proliferation resulting in a decrease in cell growth of natural killer cells and T cells. Furthermore, metabolites such as L-kynurenine have been shown to inhibit proliferation of melanoma cells in vitro. Considering these metabolite properties, the present study aimed to explore the in vitro effects of L-kynurenine, quinolinic acid and kynurenic acid on endothelioma sEnd-2 cells and on endothelial (EA. hy926 cells) (control cell line). The in vitro effect at 24, 48, and 72 h exposure to a range of 1–4 mM of the respective kynurenine metabolites on the two cell lines in terms of cell morphology, cell cycle progression and induction of apoptosis was assessed. The half inhibitory concentration (IC_{50}), as determined using nonlinear regression, for L-kynurenine, quinolinic acid and kynurenic acid was 9.17, 15.56, and 535.40 mM, respectively. Optical transmitted light differential interference contrast and hematoxylin and eosin staining revealed cells blocked in metaphase, formation of apoptotic bodies and compromised cell density in L-kynurenine-treated cells. A statistically significant increase in the number of cells present in the sub-G_1 phase was observed in L-kynurenine-treated sample. To our knowledge, this was the first in vitro study conducted to investigate the mechanism of action of kynurenine metabolites on endothelioma sEnd-2 cells. It can be concluded that L-kynurenine exerts an antiproliferative effect on the endothelioma sEnd-2 cell line by decreasing cell growth and proliferation as well as a metaphase block. These hallmarks suggest cell death via apoptosis. Further research will be conducted on L-kynurenine to assess the effect on cell adhesion in vitro and in vivo as cell-cell adhesion has been shown to increase metastasis to distant organs therefore, the inhibition of adhesion may lead to a decrease in metastasis.

KEYWORDS
apoptosis, endothelioma, kynurenic acid, L-kynurenine, quinolinic acid

1 | INTRODUCTION

Cancer is one of the leading causes of death worldwide with the major contributor to mortality being distant metastasis.[1] Epithelioid hemangioendothelioma (EHE) is an ultra-rare vascular sarcoma, usually behaving as a low-grade malignancy despite a high systemic involvement. The degree of uncertainty in selecting the most appropriate treatment of EHE patients is high, treatment options vary and the adoption of new treatments is inconsistent across the world, resulting in suboptimal outcomes for many patients.[1] Mitigation of tumour progression and metastasis play a crucial role in the development of cancer therapy.[1] Cancer tissues require oxygen and nutrients to grow, which are supplied by blood flow to the tumour.[1] The formation of new blood vessels in cancer occurs in response to various proangiogenic stimuli namely, vascular endothelial growth factor (VEGF), basic fibroblast growth factor (bFGF), placental growth factor and angiopoietin.[1] The increase in VEGF expression in the tumour microenvironment leads to continuous angiogenesis resulting in tumour blood vessels with structural defects.[1] Tumour blood vessels are highly permeable, enlarged with weakened endothelial cell junctions (ECs).[1] Hypoxia and acidity, which are associated with the tumour microenvironment also stimulate VEGF expression in tumours.[1] Hypoxia plays a crucial role in tumour aggressiveness through the epithelial-mesenchymal transition, resulting in metastasis.[1] During the first stage of metastasis, tumour cells migrate through a vascular wall, through the process of intravasation and, then travel to target organs.[2] Tumour blood vessels provide a gateway for tumour metastasis as highly vascularised tumours have an elevated metastatic potential.[2] The family of VEGF including VEGF-A, B, C, D, and E plays a role in the formation of blood vessels within a growing tumour. Consequently, VEGF proteins promote tumour growth and enable metastasis.[2,3] The increase in VEGF expression is observed in aggressive cancers and it influences the prognosis of cancer patients.[2] VEGF is one of the most potent stimulators of angiogenesis affecting EC proliferation and motility, as well as vascular permeability.[2] VEGF expression levels are upregulated by cytokines and growth factors such as fibroblast growth factor (FGF), platelet-derived growth factor (PDGF) and transforming growth factor.[2,3] VEGFs exert their angiogenic functions through activation of tyrosine kinase receptors VEGFR- 1 and VEGFR-2, which are primarily expressed by ECs. VEGFR-2 has been found to be expressed in melanoma and mesothelioma cell lines and treatment with VEGF-A resulted in increased cell proliferation via activation of VEGFR-2.[2]

Previous studies have shown that tumour ECs (TECs) differ from normal ECs in their angiogenic properties, gene expression profiles and responses to growth factors and chemotherapeutic drugs.[2,4,5]

Vasculature in non-diseased organs has an organised hierarchical structure that supports the efficient distribution of blood and its components to cells.[1] TECs that cover the inner surfaces of tumour blood vessels are the primary targets of antiangiogenic therapy. The TECs show intertumoral and intratumoral heterogeneity when communicating with the tumour microenvironment resulting in resistance to antiangiogenic therapy.[1,2] Antiangiogenic therapy was proposed by Dr. Folkman, he suggested that preventing neovascularisation could decrease tumour growth to a very small diameter of 2–3 mm.[1,4,5] Angiogenic inhibitors such as bevacizumab, a human anti-VEGF antibody has been used to suppress tumour growth, improve the structure of blood vessels and increase delivery of oxygen and drugs which will affect radiotherapy and chemotherapy.[1,2] However, the clinical benefits of antiangiogenic therapies are limited, this may result in an improvement of the prognosis such as progression-free survival. Resistance to antiangiogenic therapy has emerged because of the complex interaction between tumour cells and stromal cells which allow tumour cells to escape these targeted therapies.[1,2] Mesenchymal stromal cells (MSCs) play a crucial role in cell survival and proliferation. MSCs are able to modulate the immune response through paracrine signaling. The paracrine signaling includes secretion of small molecules such as growth factors, cytokines and chemokines. The growth factors include VEGF, insulin-like growth factor 1, epidermal growth factor and PDGF. The expression of these growth factors may lead to cell proliferation and differentiation.[1,2]

The kynurenine pathway is a major catabolic pathway of L-tryptophan in mammals, however, further research is needed since abnormalities in the kynurenine pathway have been associated with hypertension, chronic kidney diseases and cancer.[6] Kynurenine metabolites including L-kynurenine (L-kyn), 3-hydroxykynurenine, 3-hydroxyanthranilic acid and quinolinic acid (Quin) have been shown to inhibit T cell proliferation resulting in a decrease in cell growth of natural killer (NK) cells and T cells.[6,7] Tryptophan depletion induces

Significance statement

Kynurenine metabolites have been shown to inhibit cell proliferation in melanoma cells, however the effect of kynurenine metabolites on cell morphology and proliferation has not been previously investigated in endothelioma cells. Cell morphology was investigated using light microscopy, it revealed the formation of apoptotic bodies and metaphase block in L-kynurenine-treated sample. A statistically significant increase in the sub-G_1 phase of cell cycle was observed in endothelioma cells treated with L-kynurenine. L-kynurenine was identified as a promising antiproliferative kynurenine metabolite. The antiproliferative effect of L-kynurenine has not been previously reported in endothelioma.

effector T cells to undergo a G_1 cell cycle arrest and triggers an integrated stress response pathway that involves general control non repressed 2 signaling and eukaryotic initiation factor 2α phosphorylation.[8] In addition to the tryptophan depletion theory, the tryptophan utilisation theory explains that the kynurenine metabolites produced from tryptophan degradation in the kynurenine pathway might act as active substances to induce cell death. Previous studies reported that many of these kynurenine metabolites also induce immune cell death by inhibiting T-cell proliferation and promoting apoptosis.[9] High number of tumour-infiltrating T cells predicts better prognosis of cancers.[6] NK cells and cytotoxic T cells can identify and destroy immunogenic cancer cells, especially in early stages of cancer.[6] Tumour cells promote differentiation of T Regulatory cells to prevent the cytotoxic activity of competent immune cells.[6] Moreover, potentiation of immune response improves cancer chemotherapy.[6] Furthermore, kynurenine increases invasion, metastasis and chemoresistance in specific cancer cells.[10] A randomized double-blind study phase 3 trial investigated the effect of Epacadostat, an indolamine 2,3 dioxygenase (IDO) 1 selective inhibitor and they showed that Epacadostat (100 mg) administered twice daily in combination with pembrolizumab did not improve survival in patients with metastatic melanoma.[11] Tumour IDO is involved in vascularization. In murine metastasised melanoma, IDO expression has been associated with upregulation of VEGF-C expression which induces lymphangiogenesis, which is may be linked to metastasis to the lymph node.[12] Furthermore, IDO expression has been proposed to stimulate metastasis; a correlation between IDO overexpression at the primary tumour and the development of lymph nodes metastases has been reported in various malignancies.[12] The kynurenine pathway is initiated by the conversion of L-tryptophan to formyl-kynurenine by two rate-limiting enzymes, namely tryptophan-2,3 dioxygenase (TDO) and IDO.[6] This IDO activity correlates with tumour progression and may facilitate tumour metastasis. It has been shown that IDO is overexpressed at an early stage of cancer and it is associated with poor prognosis in many tumours including endometrial, cervical, oesophageal, gastric, colon, hepatocarcinoma, and melanoma.[6] In a study by Lyon and colleagues, it was concluded that there was a significant increase in IDO expression in patients with early-stage breast cancer when compared to the controls.[13] A lower serum concentration of tryptophan and a higher kynurenine concentration which resulted in a higher kynurenine/tryptophan ratio have been observed in cancer patients.[6,13] Previous research showed the antiproliferative effect of L-kyn on human melanoma A375 cells. L-kyn also showed a cytotoxic effect on melanoma cells as it increased lactate dehydrogenase (LDH) release. L-kyn significantly induced apoptosis which was visualized by Hoescht 33342 and propidium iodide staining.[10]

Stress-induced activation of the hypothalamic pituitary adrenal axis results in the release of glucocorticoids from the adrenals which can lead to the induction of TDO upon activation of intracellular glucocorticoid receptors (GR). TDO subsequently metabolises tryptophan to kynurenine, which is then converted to either kynurenic acid (KA) by kynurenine aminotransferase or 3-hydroxykynurenine by kynurenine monooxygenase. It has been shown that L-kynurenine reacts with hydroxyl radical resulting in the formation of Kynurenic acid which decreases DNA and protein degradation.[14] Schlichtner et al. reported that L-kynurenine inhibited T cell function as an aryl hydrocarbon receptor ligand.[15] The mechanisms through which L-kynurenine suppresses T cell function is still unclear however, a possible mechanism of action is that the breakdown of L-tryptophan is required for the T cells to function. It has been shown that tryptophan expression is not inhibited when L-kynurenine expression is upregulated and L-kynurenine may be involved in immunological tolerance.[15–17]

The aim of this study was to investigate the possible anticancer effects of kynurenine metabolites, namely L-kyn, Quin and kynurenic acid (KA) on endothelioma sEnd-2 cells. The kynurenine metabolites' potential anticancer properties were investigated by means of cycle progression and apoptosis induction in endothelioma cells.

2 | MATERIALS AND METHODS

2.1 | Ethics approval

Ethical approval has been granted to conduct this study by the University of Pretoria Ethics Committee. Ethics number 283/2021.

2.2 | Endothelioma cell line

The mouse primary vein ECs (C57BL/6-GFP) were isolated from the inferior vena cava of pathogen-free C57BL/6 mice.[18,19] These sEnd-2 cells were kindly provided by Professor M Pepper from the Institute of Cellular and Molecular Medicine at the University of Pretoria, Pretoria, South Africa. The endothelioma cells were grown in high glucose Dulbecco's Modified Eagle Medium (DMEM) supplemented with 10% fetal bovine serum, 2 mM glutamine and 20 µg/mL penicillin streptomycin and fungizone.

2.3 | Human vascular ECs

The human EC line (EA. hy926) was derived from human umbilical vein and possess characteristics of vascular ECs; the cells were obtained from the American Type Culture Collection (ATCC) and were used until passage 100 since it has been reported that EA. hy926 maintain identical characteristics for 100 passages. EA. hy926 were cultured in DMEM supplemented with 10% fetal bovine serum and 1% penicillin/streptomycin in a humidified environment atmosphere of 5% CO_2 at 37°C.

2.4 | Kynurenine metabolites

L-kyn, Quin and KA were purchased from Merck, catalogue numbers K8625, P6,320-4, and K3375-1G respectively. The metabolites were

separately dissolved in 0.1 M phosphate buffered saline (PBS) containing dimethyl sulphoxide (DMSO) with a final concentration not exceeding 0.2% (v/v) at a concentration of 250 mM stock solutions for L-kyn and Quin and at a concentration of 100 mM stock solution for KA. The cells were treated with the respective metabolites at concentrations of 1–4 mM for 24, 48, and 72 h.

2.5 | General laboratory reagents and cell culture procedures

DMEM was obtained from Whitehead Scientific, Brackenfell, Cape Town, South Africa. Penicillin, DMSO, trypan blue, RNase A and Bouin's fixative were obtained from Merck.

The sEnd-2 cells and EA. hy926 cells were maintained according to the cell culture protocol specified by literature.[10,18,19] Cells were grown from cryopreserved stocks stored in freeze medium made up of 80% (v/v) FCS, 10% (v/v) DMSO and 10% (v/v) DMEM. Once the cells reached 80% confluency, they were detached by removing growth medium and washed with sterile X1 PBS (5 mL). Thereafter, the sEnd-2 cells were incubated in 5% (w/v) Trypsin in 0.1 M PBS for 10–20 min and the EA. hy926 cells were incubated in Tryple express (1 mM EDTA) for approximately 5–10 min until they appeared round and detached. Fresh medium was added to the detached cells and they were either divided into subcultures, used in experiments or frozen away in cryotubes at −80°C in a freezer.

All the cell culture procedures were performed in a sterile environment while applying aseptic techniques throughout, with all work being conducted in a laminar flow cabinet from Labotec. Solutions were sterilised using filters (0.22 µm pore size and manufactured by GVS Filter Technologies) and all glassware and pipette tips were autoclaved (20 min, 120°C, 15 psi) using the Steriliser Technologies Autoclave A2462, Linden, Germany.

2.6 | Spectrophotometry

2.6.1 | Crystal violet staining

sEnd-2 cells and EA. hy926 cells were seeded in 96 well tissue culture plates at a cell density of 5000 cells per well. Cells were then incubated overnight at 37°C, 5% CO_2 for 24 h to allow for attachment. Cells were subsequently exposed to concentrations of 1, 2, 3, and 4 mM for each of the kynurenine metabolites for 24, 48, and 72 h respectively at 37°C. After exposure, cells were fixed with 100 µL of 1% glutaraldehyde (incubation for 30 min at 37°C). Subsequently, glutaraldehyde was discarded and cells were stained using 0.1% (100 µL) crystal violet (incubated at room temperature for 30 min). The crystal violet solution was discarded and the 96 well plate was submersed under running water to remove any excess staining. The plates were left to dry overnight and the crystal violet dye was solubilised using 10% (100 µL) acetic acid and incubated at room temperature for 30 min. The absorbance of the 96-well plate was read at 570 nm using an ELx800 Universal Microplate Reader (Bio-Tek Instruments Inc.) and results were reported as percentage cell number in relation to the vehicle control. The IC_{50} was determined from the percentage cell number data using nonlinear regression via the Graph Pad Prism software version 9.5.1 (2023).

2.7 | Light microscopy

2.7.1 | Polarised optical transmitted light differential interference contrast

sEnd-2 cells were seeded at a density of 3500 cells per well in 24-well plates. EA. hy926 cells were seeded at a density of 5000 cells per well. The seeding densities differ due to the population doubling times of the two cell lines. The doubling time of EC lines is 25 h while the doubling time of immortalized endothelioma cell lines is 15 h.[20] The cells were incubated overnight to allow for attachment and they were exposed to kynurenine metabolites (Quin and L-kyn) at IC_{50} concentrations for 48 h. Polarisation-optical differential interference (PlasDIC) images were taken using the Zeiss Axiovert-40 microscope (Zeiss).

2.7.2 | Haematoxylin and eosin (H&E) staining

sEnd-2 cells were seeded at a density of 3500 cells per well in 24-well plates on heat-sterilised coverslips. EA. hy926 ECs were seeded at a density of 5000 cells per well. The cells were incubated overnight to allow for attachment and they were exposed to the kynurenine metabolites (Quin and L-kyn) at IC_{50} concentrations for 48 h. Cells were fixed in Bouin's fixative for an hour at room temperature. The fixative was discarded and 70% (v/v) ethanol was added and was incubated for a period of 20 min. The coverslips were then rinsed with tap water before the haematoxylin was added and left for a period of 20 min. After rinsing thrice for 5 min each with tap water, coverslips were washed with 70% ethanol and stained with eosin for 5 min. Coverslips were dehydrated in a stepwise manner using 70% ethanol twice for 5 min, 96% ethanol twice for 5 min, 100% ethanol twice for 5 min and xylol for 5 min after which they were mounted on microscope slides using resin to allow for permanent attachment onto the slides and left to dry overnight. The photomicrographs were taken using a Zeiss Axio Imager M2 (Zeiss).

2.8 | Flow cytometry

2.8.1 | Cell cycle analysis

sEnd-2 and EA. hy926 cells were seeded at a density of 1×10^6 cells in T25 tissue culture flaks and were left overnight to attach. The cells

were exposed to kynurenine metabolites (Quin and L-kyn) at IC_{50} concentrations for 48 h. Cell cycle analysis was performed using FC500 flow cytometer (Beckman Coulter, South Africa [PTY] Ltd.), to investigate the DNA content and to determine cell cycle distribution, G_2/M block and the presence of a sub-G_1 apoptotic peak, after treatment with each kynurenine metabolite.

2.8.2 | Annexin V-fluorescein isothiocyanate (FITC)/propidium iodide detection

The induction of apoptosis was evaluated and quantified by means of flow cytometry in combination with Annexin V-FITC and propidium iodide staining. Externalisation of the membrane phospholipid phosphatidylserine (PS) layer of the plasma membrane is one of the earliest indications of apoptosis.[21] Apoptotic cells with exposed PS molecules bind Annexin V, while necrotic cells characterised by compromised membranes take up propidium iodide (PI) staining. Once exposed to the extracellular environment, binding sites on PS become available for Annexin V, a 35-36 kDa, calcium (Ca^{2+})-dependent, phospholipid binding protein with a high affinity for PS.[21] Annexin V-FITC binds in the presence of calcium ions with high affinity to the negatively charged phospholipids including PS. Viable cells dependent phospholipid activity is activated resulting in the externalisation of the PS layer of the cell membrane.[18] Viable cells preserve an asymmetric division of several phospholipids between inner-and outer leaflets of the plasma membrane.[21] Four different populations of cells were identified: the viable cells (cells that are unlabeled), the early apoptotic cells (cells that bound Annexin V staining only), the late apoptotic cells (cells labelled with PI) and necrotic cells (cells bound with both Annexin V and that have been labelled with PI).[22]

The sEnd-2 cells and EA. hy926 cells were seeded in T25 cell culture flasks at a density of 1×10^6 per flask and left overnight to attach. Cells were treated with kynurenine metabolites at IC_{50} concentrations for 48 h. The cells were then washed in 0.1 M PBS, followed by centrifugation and resuspension in X1 binding buffer. Annexin V- FITC (1 µL) together with 1.5 µL of propidium iodide were added to the samples and then incubated for 5 min protected from light. Annexin V was measured using a FC500 flow cytometer (Beckman Coulter, South Africa [PTY] Ltd.)

3 | STATISTICAL ANALYSIS

All the experimental results were expressed as the mean ± standard error of the mean of triplicate samples. Significant differences between groups were calculated by one-way factorial analysis of variance (ANOVA) and $p < .05$ was considered statistically significant. For flow cytometry data, differences between controls (vehicle and positive) and experimental groups were analysed using one-way ANOVA. $^*p < .05$, $^{**}p < .01$.

4 | RESULTS

4.1 | Crystal violet staining of sEnd-2 and EA. hy926 cells treated with L-kynurenine, quinolinic acid and kynurenic acid

The effect of L-kyn, Quin and KA on cell proliferation was assessed at concentrations ranging from 1 to 4 mM using crystal violet and the absorbance was obtained to determine the percentage cell viability in sEnd-2 cells and EA. hy926 cells after 24, 48, and 72 h. A statistically significant decrease in cell number exposed to L-kyn (4 mM) and nocodazole (NOC), a microtubule inhibitor, was observed when compared to the vehicle-treated sample ($p < .05$) at 24, 48, and 72 h (Figure 1). A decrease in cell number was observed at 4 mM L-kyn-treated EA. hy926 although not statistically significant (Figure 2). The IC_{50} determined by nonlinear regression was found to be 9.17, 15.56, and 535.40 mM for L-kyn, Quin and KA respectively. For the EA. hy926, the IC_{50} was determined to be 10.93, 38.95, and 677.90 mM for L-kyn, Quin and KA respectively. Taking into consideration the elevated IC_{50} obtained for KA, the compound was excluded from further experiments conducted.

4.2 | Polarised optical transmitted light differential interference contrast images of cells treated with L-kynurenine and quinolinic acid

PlasDIC images of sEnd-2 cells treated at IC_{50} concentrations, 9.17 mM for L-kyn and 15.56 mM for Quin for 48 h revealed a compromised cell density (Figure 3). Sample treated with L-kyn showed the formation of rounded shrunken cells and NOC-treated samples showed the formation of apoptotic bodies.

PlasDIC images of EA. hy926 cells treated at IC_{50} concentrations, 9.17 mM for L-kyn and 15.56 mM for Quin for 48 h revealed a compromised cell density (Figure 4). Sample treated with L-kyn showed the formation of apoptotic bodies, as well as compromised cell density and lipid droplets formation. NOC-treated samples revealed the formation of apoptotic bodies and a decrease in cell density.

4.3 | H&E staining of L-kynurenine- and quinolinic acid-treated sEnd-2 and EA. hy926 cells

H&E staining allows for the assessment of morphological characteristics of the cytoplasm and nuclear components of the cells. The staining was used to visualise morphological changes in sEnd-2 cells after exposure to L-kyn and Quin and the appropriate controls. Cells propagated in the vehicle control (Figure 5A) showed normal cell morphology with the majority of the cells being in interphase. L-kyn-treated sample (Figure 5B) showed cells blocked in metaphase. Cells treated with Quin showed a decrease in cell density (Figure 5C)

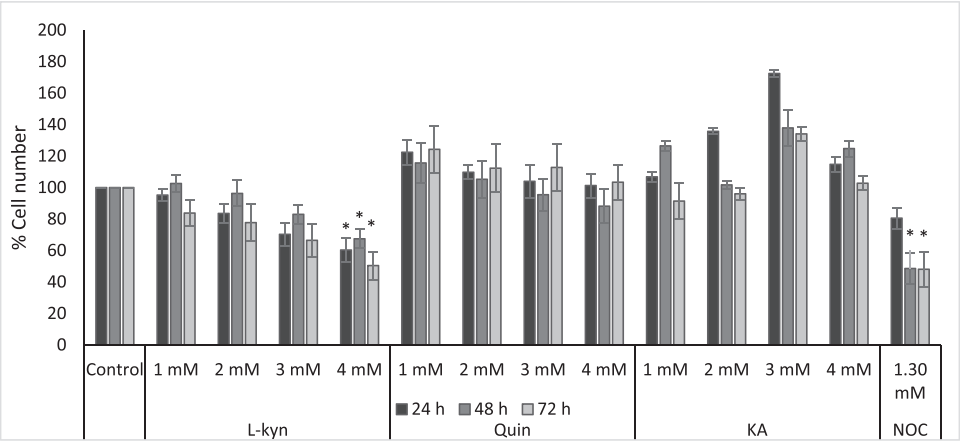

FIGURE 1 Graph representing the percentage cell number of sEnd-2 cells treated with L-kyn, Quin and KA after 24 h (black), 48 h (darker grey), and 72 h (light grey). *$p < .05$ in L-kyn- and NOC-treated samples when compared to control. NOC, nocodazole.

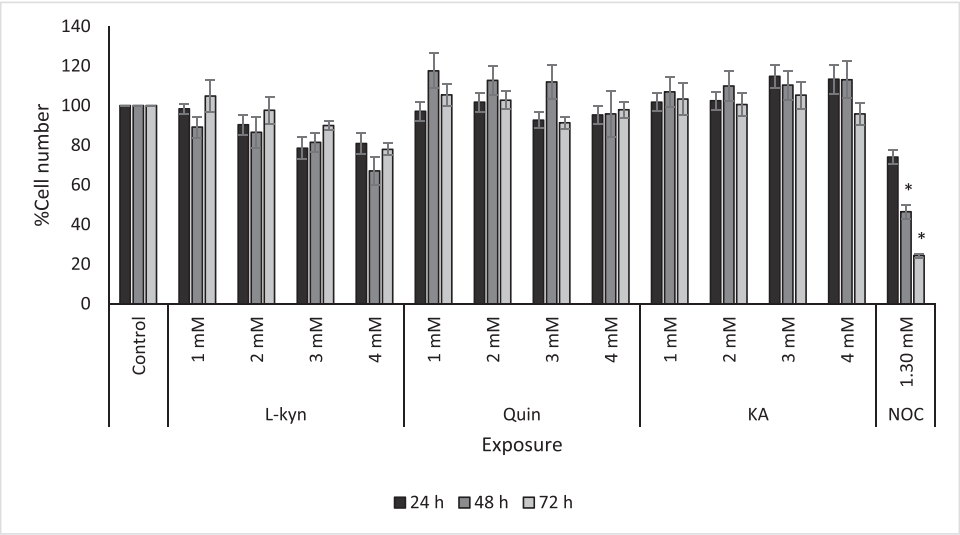

FIGURE 2 Graph representing the percentage cell number of EA. hy926 cells treated with L-kyn, Quin and KA after 24 h (black), 48 h (darker grey), and 72 h (light grey). *$p < .05$ in NOC-treated samples when compared to control. NOC, nocodazole.

and the positive control, NOC-treated cells showed rounded, shrunken cells and a decrease in cell viability (Figure 5D).

H&E staining of EA. hy926 cells at IC_{50} concentrations for L-kyn and Quin showed a decrease in cell density and formation of lipid droplets in L-kyn- and NOC-treated sample (Figures 6B,D) when compared to the vehicle control sample.

4.4 | Cell cycle analysis of cells treated with L-kynurenine and quinolinic acid

Flow cytometric analysis revealed a statistically significant increase in sEnd-2 cells and EA. hy926 cells in sub-G_1 phase (indicative of apoptosis) in the L-kyn-, Quin- and NOC-treated samples in comparison to the vehicle control after 48 h. A decrease in the G_1 phase was also observed in the NOC-treated sample when compared to the vehicle control. The bar graphs represent the percentage of sEnd-2 cells and EA. hy926 cells in different cell cycle phases, thus confirming the qualitative data observed in the PlasDIC and H&E images (Figures 7 and 8). The representative histograms of cell cycle analysis of sEnd-2 and EA. hy926 cells are represented in Figures 1 and 2, respectively, of the Supporting Information Materials.

4.5 | Apoptosis induction via Annexin V/propidium iodide staining in the L-kynurenine-and quinolinic acid-treated sEnd-2 and EA. hy926 cells

Annexin V-FITC, an apoptosis detecting assay, was used investigate the induction of apoptosis in sEnd-2 cells. Results revealed a statistically significant increase in cells in early apoptosis (56.46%) in the NOC-treated sample when compared to the vehicle control

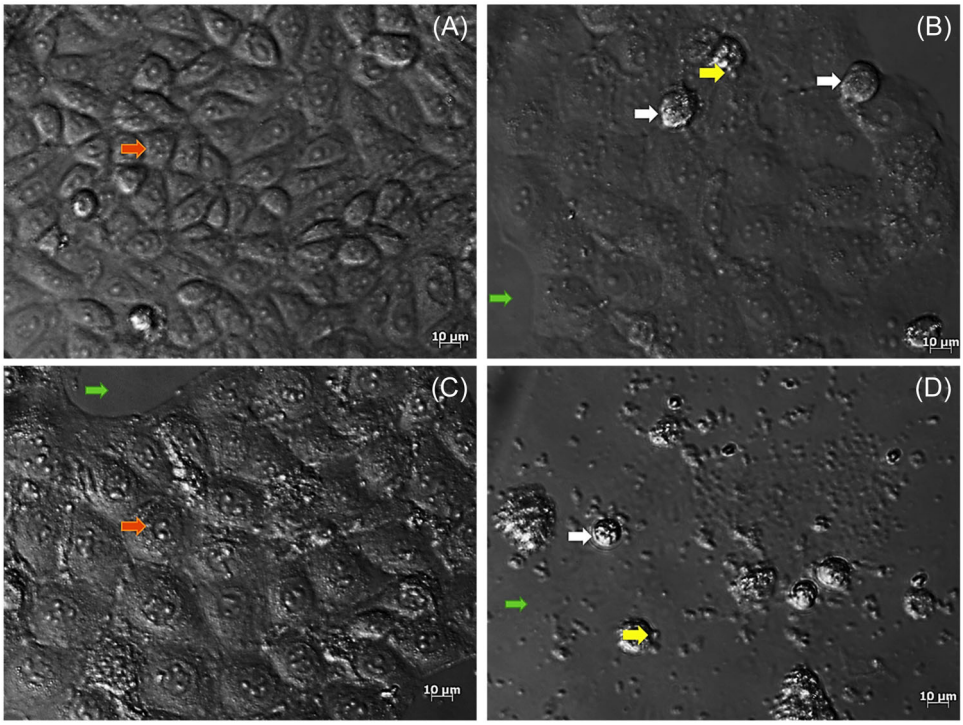

FIGURE 3 PlasDIC images of sEnd-2 cells (x40 magnification) after treatment with 9.17 mM L-kyn and 15.56 mM Quin after 48 h. (A) vehicle control, (B) L-kyn, (C) Quin, (D) NOC. Orange arrow represents interphase, green arrows indicate compromised cell density, yellow arrows represent apoptotic bodies and white arrows show rounded cells. NOC, nocodazole.

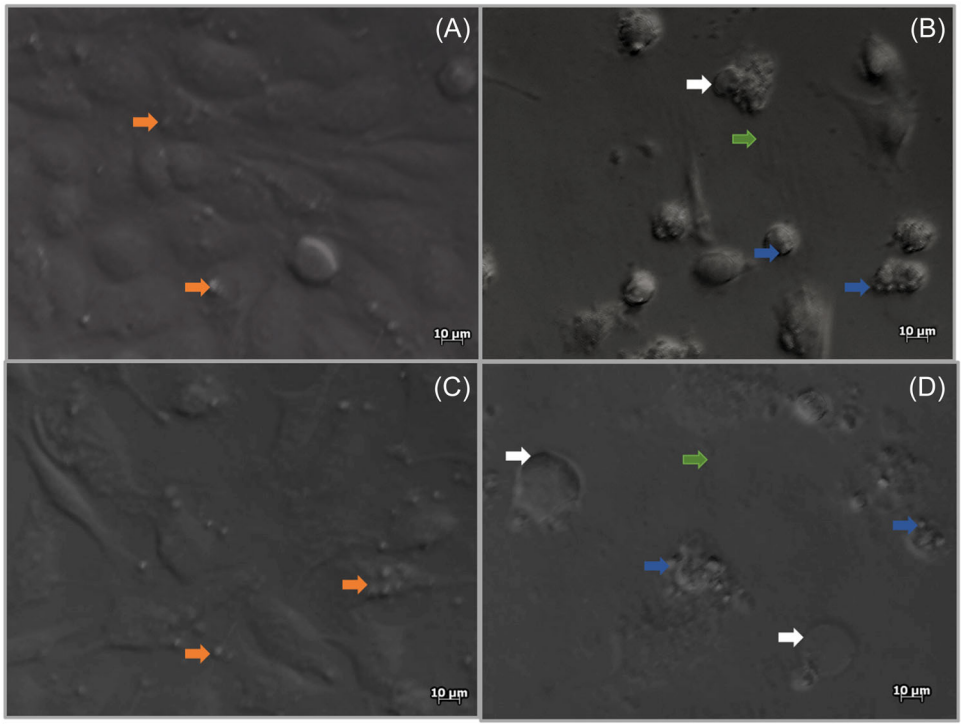

FIGURE 4 PlasDIC images of EA. hy926 cells (x40 magnification) after treatment with 9.17 mM L-kyn and 15.56 mM Quin after 48 h. (A) vehicle control, (B) L-kyn, (C) Quin, (D) NOC. Orange arrow represents interphase, green arrows indicate compromised cell density, blue arrows represent apoptotic bodies and white arrows show lipid droplets. NOC, nocodazole.

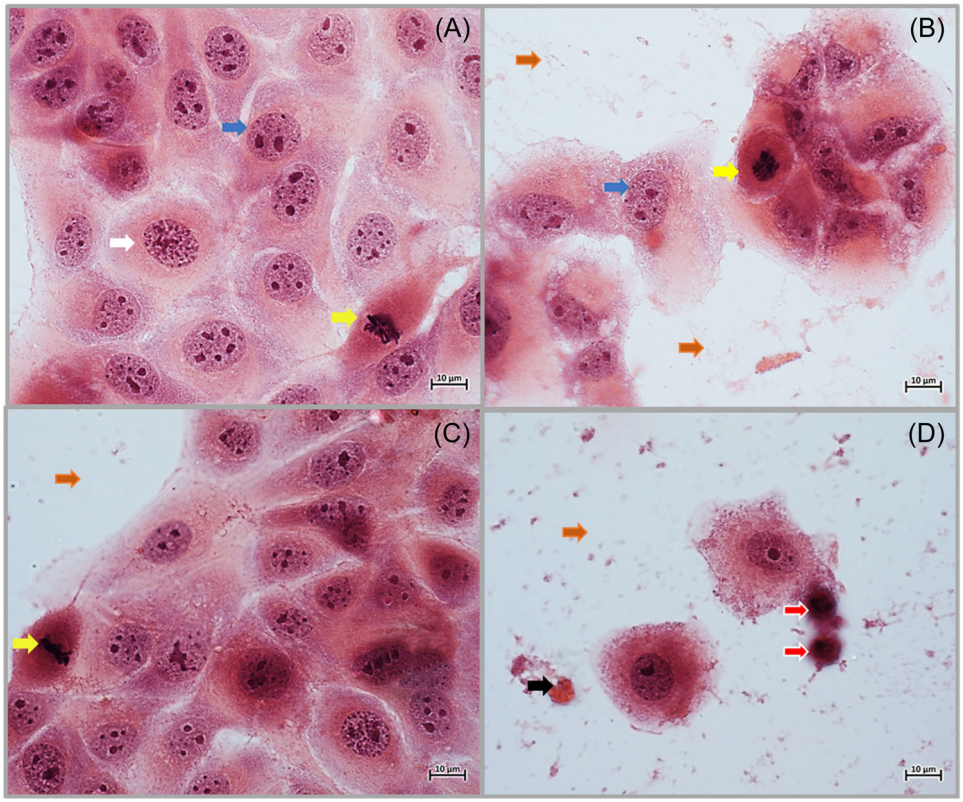

FIGURE 5 Haematoxylin and eosin staining of sEnd-2 cells treated with 9.17 mM L-kyn and 15.56 mM Quin. (A) vehicle control, (B) L-kyn, (C) Quin and (D) NOC. Yellow arrows represent metaphase block, blue arrows represent cells in interphase, orange arrows represent reduced cell density and white arrow indicates cell in prophase, black arrow shows cell debris and red arrows represent rounded shrunken cells. The images were captured at x100 magnification. NOC, nocodazole.

(5.49%) (Figure 9) ($p < .01$). Actinomycin D (0.1 µg/mL) was used as a positive control and it showed a 5.85% increase in cells in early apoptosis. However, the increase was not statistically significant.

A statistically significant increase in cells in late apoptosis in the NOC-treated cells (17.88%) was observed when compared to the vehicle control (0.61%) in EA. hy926 cells (Figure 10) ($p < .05$). Dot plots of sEnd-2 and EA. hy926 cells showing viable cells, cells in early apoptosis, cells in late apoptosis and necrotic cells are represented in Figures 3 and 4, respectively, of the Supporting Information Materials.

5 | DISCUSSION

In this study, crystal violet staining was used to investigate the effect of L-kyn, Quin and KA on cell proliferation. The staining is directly proportional to the cell biomass that is attached in the cell culture plate. The cell biomass may be used to infer the percentage of cell viability, however crystal violet does not provide insight into the type of cell death. Therefore, other assays such as Annexin V are conducted to confirm the nature of the cell death.[23] KA did not induce a decrease in cell proliferation of endothelioma in vitro which is the reason why it was excluded from further experiments conducted. Previous studies reported a more potent antiproliferative effect measured by means of 3-(4,5-dimethylthiazol-2-yl)−2,5-diphenyl-2H-tetrazolium bromide (MTT) assay rather than the crystal violet assay.[24,25] The difference may result from the mechanism of biological activity of KA since MTT determines metabolic activity of cells whereas crystal violet determines DNA content.

In agreement with this current study, a study by Walczak et al. revealed that L-kyn, but not KA, exerted antiproliferative effects on human melanoma A375 and RPMI7951 cells at millimolar concentration.[26] Although in the current study, the L-kyn IC_{50} of 9.17 mM was high, literature has shown that a L-kynurenine has a biological range of 0.1 mM − 5 mM and 5 mM was shown to be cytotoxic to cells.[27] Furthermore Opitz et al. showed that L-kynurenine (5 mM) induced DNA damage in melanoma A375 cells after 24 h of exposure.[28] L-kynurenine cytotoxicity was tested on melanoma A375 cells by LDH assay and they observed a statistically significant increase in LDH release showing the strong antiproliferative effect of L-kynurenine at 5 mM on melanoma A375 cells,[26] they also reported that L-kynurenine inhibited cell proliferation of melanoma RPMI7951 cells at a concentration of 5 mM[26] The authors also investigated the cytotoxicity of L-kyn and KA on human melanocytes (HEMa) and melanoma RPMI7951 cells by means of LDH assay. They showed that L-kyn and KA did not induce cytotoxicity in melanocyte cells

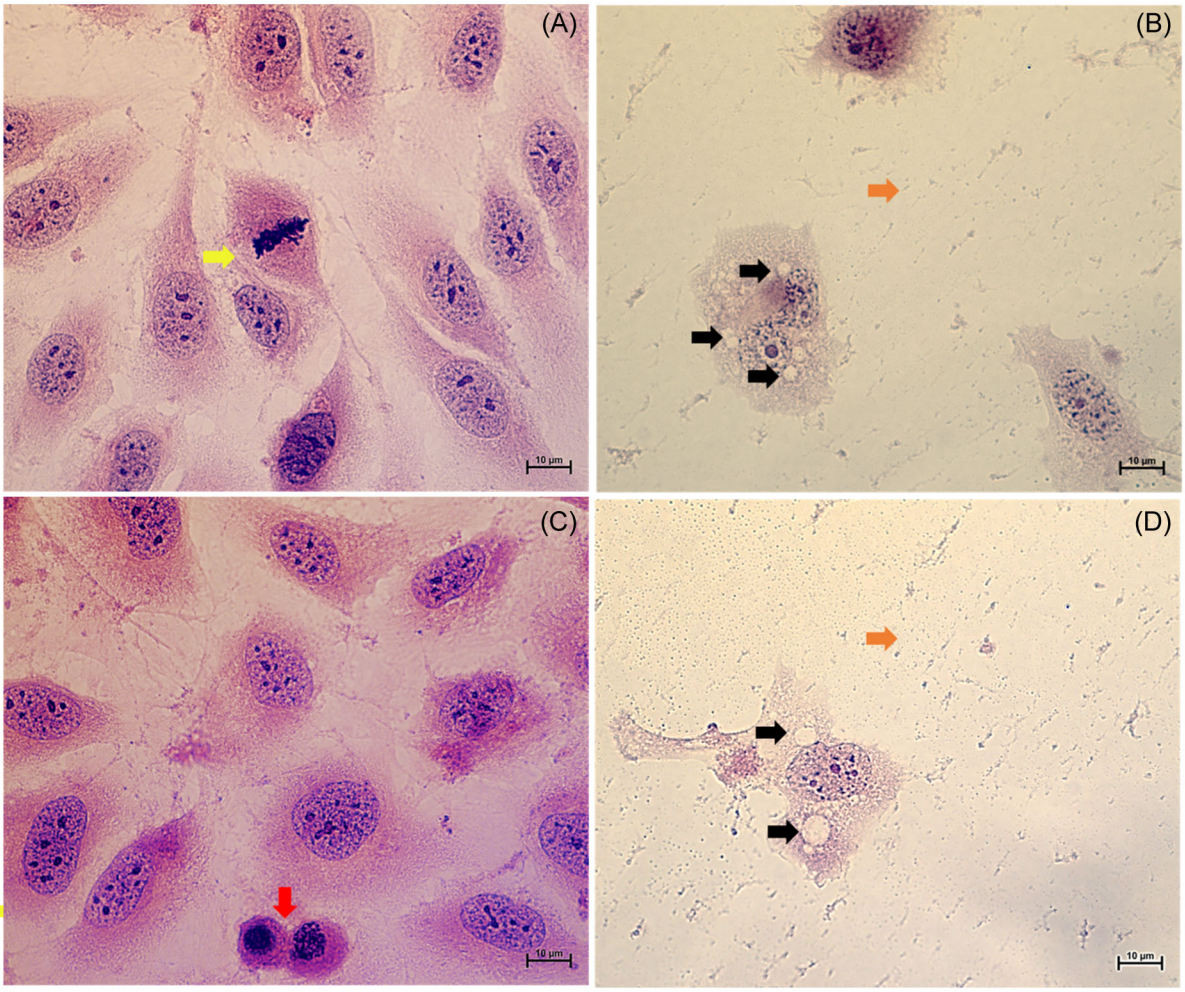

FIGURE 6 Haematoxylin and eosin staining of EA. hy926 cells treated with 9.17 mM L-kyn and 15.56 mM Quin. (A) vehicle control, (B) L-kyn, (C) Quin and (D) NOC. Yellow arrows represent metaphase block, orange arrows represent reduced cell density, black arrow shows lipid droplets and the red arrow represents cells in telophase. The images were captured at x100 magnification. NOC, nocodazole.

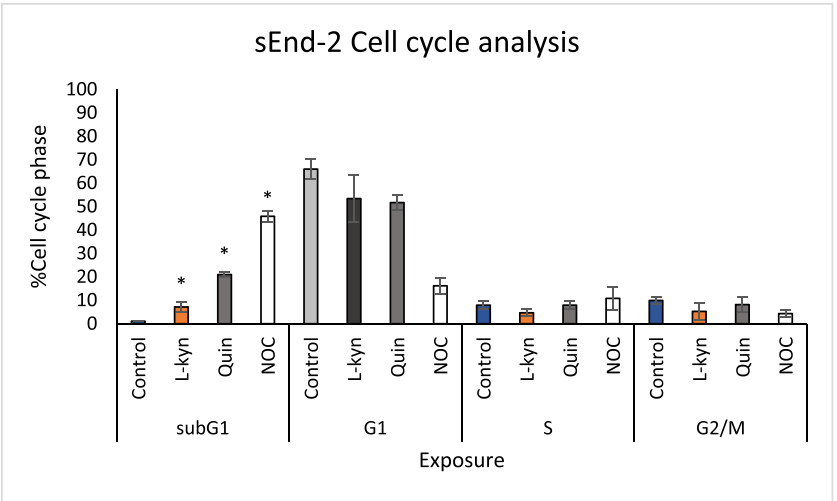

FIGURE 7 Bar graph quantifying the percentage of sEnd-2 cells in sub-G_1, G_1, S, and G_2 phases for control (blue), L-kyn (orange), Quin (grey) and NOC (white). *$p < .05$ compared to the control of each phase. NOC, nocodazole.

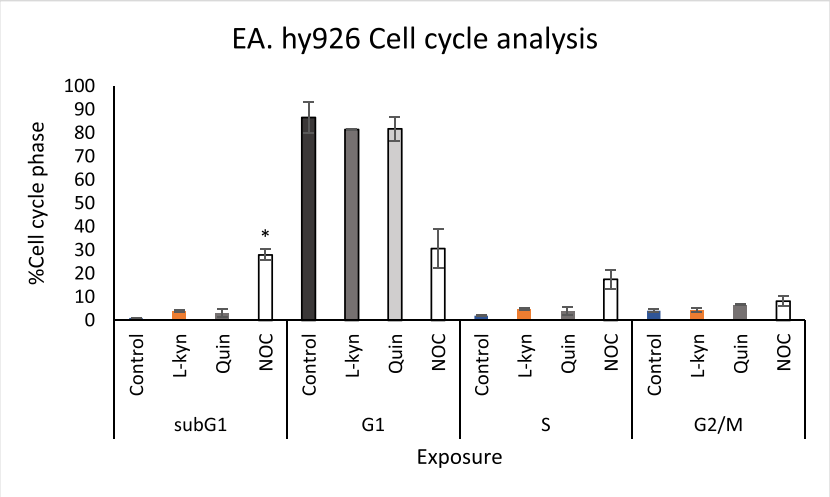

FIGURE 8 Bar graph quantifying the percentage of EA. hy926 cells in sub-G_1, G_1, S and G2 phases for control (blue), L-kyn (orange), Quin (grey) and NOC (white). *$p < .05$ compared to the control of each phase. NOC, nocodazole.

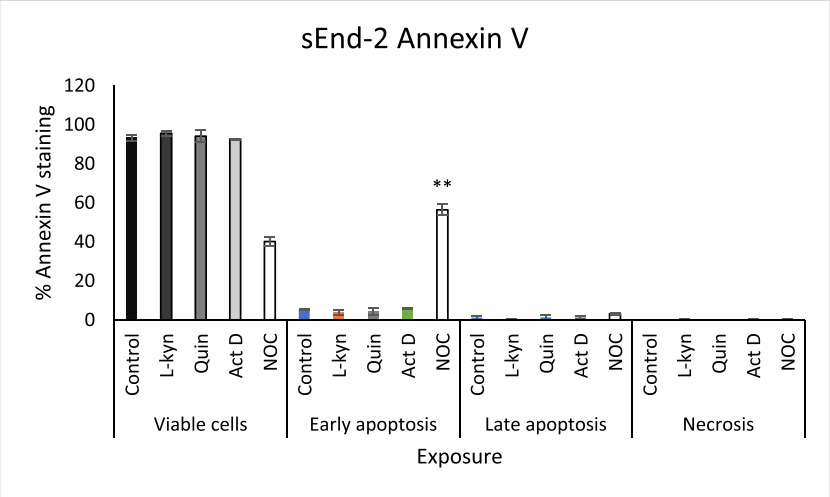

FIGURE 9 Bar graph representing percentage Annexin V staining sEnd-2 cells. Vehicle control (blue), L-kyn (orange), Quin (grey), Act D (green) and NOC (white), **$p < .01$ compared to the control of each phase. NOC, nocodazole.

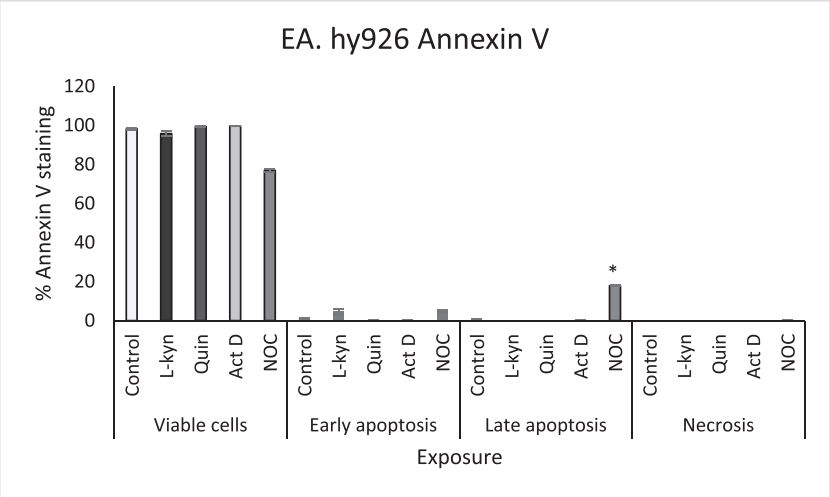

FIGURE 10 Bar graph representing percentage Annexin V staining EA. hy926 cells. Vehicle control (blue), L-kyn (orange), Quin (grey), Act D (green) and NOC (white), *$p < 0.05$ compared to the control of each phase. NOC, nocodazole.

whereas cytotoxicity was induced in melanoma A375 cells as evidenced by an increase in LDH release in the melanoma cells.[26] The first-in-human study of L-kynurenine showed that L-kynurenine was safe and well-tolerated after intravenous infusion up to 5 mg/kg in human participants.[29] Another study conducted by Thaker et al. investigated the effect of quinolinic acid on cell proliferation of human colorectal adenocarcinoma cells (HT-19); they observed no change in cell proliferation.[30] Similar findings were reported by Trott

and colleagues who concluded that Quin did not affect cell proliferation in renal cell carcinoma.[31] A study by Buchanan et al. revealed a 50% decrease in cell proliferation in human colon cancer cells (HCT 116) after treatment with 3-hydroxykynurenine (3-HK) at a concentration of 2 mM for 48 h.[32] Consistent with these findings, this current study showed antiproliferative effects on endothelioma cells at a concentration of 4 mM after 24, 48, and 72 h as seen with a statistically significant decrease in cell proliferation when compared to the vehicle control ($p < .05$).

NOC was used as a positive control because literature showed that it is a microtubule de-polymerizing agent, it causes mitotic arrest at the sub G_1 phase of cell division which is followed by the induction of apoptosis.[33] This is in agreement with this current study where we observed an increase in the percentage of cells in the sub G_1 phase in NOC-treated samples and the induction of apoptosis was confirmed by cell morphology namely compromised cell density and the formation of apoptotic bodies as well as by a statistically significant increase Annexin V staining in the NOC-treated sample shown compared to the vehicle control. The NOC-treated sample also showed a statistically significant decrease in cell proliferation in the endothelioma sEnd-2 cells after 48 and 72 h of exposure. Similar findings were observed in EA. hy926 cells namely, a decrease in cell proliferation (not statistically significant) which was confirmed by cell morphology, PlasDIC and H&E staining in L-kyn-treated samples when compared to the vehicle control.

Qualitative results obtained via PlasDIC and H&E staining revealed the formation of apoptotic bodies, rounded cells and cells blocked in metaphase in the L-kyn-treated sample at the IC_{50} concentration previously determined. The morphology studies support the findings of the quantitative results that indicate the induction of apoptosis as seen with the increase in the number of cells in sub-G_1 in cells treated with L-kyn ($p < .05$), suggesting cell death by apoptosis. However, Annexin V-FITC apoptosis-detection assay showed an increase, although non-statistically significant in cells in early apoptosis in the L-kyn-treated sample.

In a study by Song et al. the induction of apoptosis after treatment with L-kyn in human NK (NK92 MI) cells for 24 h showed an increase in annexin V-positive cells suggesting an increase in the number of cells undergoing apoptosis. The effect of L-kyn on cell cycle progression revealed an increase in cell cycle arrest at G_0–G_1 phase, however the increase was not statistically significant. Therefore, Song and colleagues concluded that L-kyn inhibits cell growth, but does not interfere with cell cycle arrest.[34] In this current study, a statistically significant increase was observed in the sub-G_1 phase in the L-kyn-treated endothelioma cells and the annexin V-positive did not show a significant increase after treatment with L-kyn. This current study's findings differ from the results obtained by Song et al. These differences may be explained by the fact that in the study by Song and colleagues, the cells were treated with L-kyn for 24 h and the cells may still be in early apoptosis which can be shown by the increase in Annexin V-positive staining but not an increase in the sub-G_1 phase. Whereas in this current study, the cells were treated with L-kyn for 48 h and an increase in cells in sub-G_1 which indicates apoptosis and an increase in cells in early apoptosis were observed, however the increase was not statistically significant which suggests that the cells may have surpassed the early apoptotic stage. In the study by Song et al. cells were treated with L-kyn for 24 h whereas in the current study, cells were exposed to L-kyn for 48 h, this may result in differences in cell cycle arrest at the sub G_1 phase observed.

The antiproliferative effect of L-kyn was investigated by crystal violet assay that showed a statistically significant decrease in percentage cell number at 4 mM L-kyn. The effect on DNA content was also assessed via cell cycle analysis where we observed a statistically significant increase in the percentage of cells in the sub-G1 phase indicative of apoptosis. Cell morphology showed compromised cell density, metaphase block and formation of apoptotic bodies, these hallmarks suggest apoptosis.

The vascular tumour derived ECs express aryl hydrocarbon receptors (AhR). It has been shown that treatment of sEnd-2 with Bleomycin (an antineoplastic drug used to treat haemangiomas) resulted in apoptosis as evidence by a decrease in antiapoptotic Bcl-2 protein as well as in increase in annexin V staining and changes in cell morphology namely membrane blebbing and nuclear fragmentation which are hallmarks associated with apoptosis.[35] In addition, L-Kynurenine is an endogenous agonist of AhR is produced enzymatically from tryptophan by indoleamine 2,3-dioxygenase (IDO) and tryptophan 2,3-dioxygenase (TDO).[36] Previous studies revealed that IDO and TDO are expressed and upregulated in various cancer types, including melanoma.[26,36]

The involvement of kynurenine metabolites was first observed in early studies in which cancer patients were reported to have higher kynurenine expression when compared to controls.[37] Cancer patients had a lower tryptophan expression and higher kynurenine metabolites in their blood and urine.[37] A study by Muller et al. revealed that combination therapy of a chemotherapeutic drug and an IDO inhibitor, 1-methyl-D-tryptophan (1MT) reduced tumour size by 30% in a mouse model.[38] The outcome of this study has paved the way to identifying kynurenine metabolites as potential targets to address cancer progression and metastasis. An elevated IDO/TDO activity has been reported in tumours and blood sampled from patients with cancer including glioblastoma, colorectal cancer, breast and liver cancer with an increase in mid-G_1 phase arrest observed in T cells.[38] Similarly, L-kyn statistically significantly increased cells in sub-G_1 in endothelioma sEnd-2 at a concentration of 9.17 mM after 48 h.

The effect of kynurenine metabolites in macrophage cells was investigated by Munn et al. and they found a cell cycle arrest at the sub-G_1 phase of T cells.[39] Similarly, an increase in sub-G_1 was observed in this current study in L-kyn-treated samples. In breast,[40,41] colorectal,[42,43] glioblastoma[28,44] and liver cancer,[45] an increase in IDO activity was observed in tumour cells when compared to controls. Although the expression of kynurenine metabolites varies depending on the cancer type, these studies highlight the crucial role of kynurenine metabolites in cancer progression.[46]

Kynurenine metabolites namely, L-kyn and Quin may constitute as potential anticancer adjunct chemotherapeutic agents, since they

have shown in this study to significantly reduce cell proliferation and induce apoptosis. Overall, our results suggest L-kyn promotes cell cycle arrest in the sub-G_1 phase and induces apoptosis in sEnd-2 and EA. hy926 cells by upregulating biomarkers associated with apoptosis and an increase in cells in early apoptosis.

6 | CONCLUSION

L-kyn induces cell death via apoptosis at a concentration of 9.17 mM in the endothelioma sEnd-2 cell line which was observed by the presence of apoptotic bodies, rounded cells and cell cycle arrest in the sub-G_1 phase. Data from this study provides novel insights into the mechanism of action of L-kyn and suggests that L-kyn represents a promising adjunct chemotherapeutic agent against endothelioma.

This study identified L-kyn as a promising antiproliferative kynurenine metabolite. Quin also showed promising antiproliferative properties however, to a lesser extent when compared to L-kyn. Future studies will investigate the mechanism of action of L-kyn on cell adhesion by quantifying adhesion proteins namely E-cadherin, Paxillin and focal adhesion kinase in vitro in melanoma cells and in vivo in murine models.

AUTHOR CONTRIBUTIONS

All experiments and data analyses were conducted by Danielle Sandra Nkandeu. Danielle Sandra Nkandeu, Anna Margaretha Joubert, Yvette Nkondo Hlophe, June Cheptoo Serem and Priyesh Bipath contributed to data interpretation. Danielle Sandra Nkandeu wrote the original draft with critical review and input from Anna Margaretha Joubert, Priyesh Bipath, June Cheptoo Serem and Yvette Nkondo Hlophe. Yvette Nkondo Hlophe, Priyesh Bipath and June Cheptoo Serem contributed to the study's conception and design. All authors have approved the final version of the manuscript and agree to be accountable for all aspects of the work in ensuring that questions related to the accuracy or integrity of any part of the work are appropriately investigated and resolved.

ACKNOWLEDGMENTS

This research was funded by grants awarded to: Dr. Yvette Nkondo Hlophe from the National Research Foundation, grant number: A1F4685 & N1F580 and to Ms Danielle Sandra Nkandeu from The University Capacity Development Programme (UCDP), grant number: A1D783 & N1F120. University of Pretoria, National Research Foundation, Grant number: A1F4685 & N1F580. The University Capacity Development Programme (UCDP), Grant number: A1D783 & N1F120.

CONFLICT OF INTEREST STATEMENT

The authors declare no conflict of interest.

DATA AVAILABILITY STATEMENT

The data that support the findings of this study are available from the corresponding author upon reasonable request.

ORCID

Danielle Sandra Nkandeu http://orcid.org/0000-0001-5881-8495
Anna Margaretha Joubert http://orcid.org/0000-0002-6931-7554
June Cheptoo Serem http://orcid.org/0000-0001-9912-166X
Priyesh Bipath http://orcid.org/0000-0002-5433-7069
Yvette Nkondo Hlophe http://orcid.org/0000-0002-3112-2436

REFERENCES

1. Maishi N, Annan DA, Kikuchi H, Hida Y, Hida K. Tumor endothelial heterogeneity in cancer progression. *Cancers*. 2019;11(10):1511. doi:10.3390/cancers.11101511
2. Maishi N, Ohba Y, Akiyama K, et al. Tumour endothelial cells in high metastatic tumours promote metastasis via epigenetic dysregulation of biglycan. *Sci Rep*. 2016;6:28039. doi:10.1038/srep28039
3. Hlophe YN, Joubert AM. Vascular endothelial growthfactor-C in activating vascular endothelial growth factor receptor-3 and chemokine receptor-4 in melanoma adhesion. *J Cell Mol Med*. 2022;26(23):5743-5754.
4. Hida K, Maishi N, Annan D, Hida Y. Contribution of tumor endothelial cells in cancer progression. *Int J Mol Sci*. 2018;19(1272):1272. doi:10.3390/ijms.19051272
5. Hida K, Maishi N. Abnormalities of tumour endothelial cells and cancer progression. *Oral Sci Int*. 2017;15:1-6.
6. Sforzini L, Nettis MA, Mondelli V, Pariante CM. Inflammation in cancer and depression: a starring role for the kynurenine pathway. *Psychopharmacology*. 2019;236:2997-3011.
7. Ciapala K, Mika J, Rojewska E. The kynurenine pathway as a potential target for neuropathic pain therapy: from basic research to clinical perspectives. *Int J Mol Sci*. 2021;22(20):11055. doi:10.3390/ijms222011055
8. Creelan BC, Antonia SJ, Bepler G, Garrett TJ, Simon GR, Soliman HH. Indoleamine 2,3-dioxygenase activity and clinical outcome following induction chemotherapy and concurrent chemoradiation in stage III non-small cell lung cancer. *OncoImmunology*. 2013;2(3):23428. doi:10.4161/onci.23428
9. Basson C, Serem JC, Hlophe YN, Bipath P. The tryptophan-kynurenine pathway in immunomodulation and cancer metastasis. *Cancer Med*. 2023;12:18691-18701.
10. Davis I, Liu A. What is the tryptophan kynurenine pathway and why is it important to neurotherapeutics? *Expert Rev Neurother*. 2015;15(7):719-721.
11. Long GV, Dummer R, Hamid O, et al. Epacadostat plus pembrolizumab versus placebo plus pembrolizumab in patients with unresectable or metastatic melanoma (ECHO-301/KEYNOTE-252): a phase 3, randomised, double-blind study. *Lancet Oncol*. 2019;20(8):1083-1097.
12. Meireson A, Devos M, Brochez L. IDO expression in cancer: different compartment, different functionality. *Front Immunol*. 2020;11:534191. doi:10.3389/fimmu.2020.531491
13. Lyon DE, Walter JM, Starkweather AR, Schubert CM, McCain NL. Tryptophan degradation in women with breast cancer: a pilot study. *BMC Res Notes*. 2011;4:156. http://www.biomedcentral.com/1756-0500/4/156
14. O'Farrell K, Harkin K. Stress-related regualtion of the kynurenine pathway: relevance to neuropsychiatric and degenerative disorders. *Neuropharmacology*. 2017;112(Pt B):307-323.
15. Schlichtner S, Yasinka IM, Klenova E, et al. L-kynurenine participates in cancer immune evasion by downregulating hypoxic signaling in T lymphocytes. *Oncoimmunology*. 2023;12(1):2244330. doi:10.1080/2162402X.2023.2244330
16. Abd el-Fattah EE. IDO/Kynurenine pathway in cancer: possible therapeutic approaches. *J Transl Med*. 2022;20(1):347. doi:10.1186/s12967-022-03554

17. Mezrich JD, Fechner JH, Zhang X, Johnson BP, Burlingham WJ, Bradfield CA. An interaction between kynurenine and the aryl hydrocarbon receptor can generate regulatory T cells. *J Immunol*. 2010;185(6):3190-3198. doi:10.4049/jimmunol.0903670
18. Mizoguchi T, Ueno K, Takeuchi Y, et al. Treatment of cutaneous ulcers with multilayered mixed sheets of autologous fibroblasts and peripheral blood mononuclear cells. *Cell Physiol Biochem*. 2018;47: 201-211.
19. Sekiguchi K, Ito Y, Hattori K, et al. VEGF receptor 1-Expressing macrophages recruited from bone marrow enhances angiogenesis in endometrial tissues. *Sci Rep*. 2019;9:7037. doi:10.1038/s41598-019-43185-8
20. Krump-Konvalinkova V, Bittinger F, Unger RE, Peters K, Lehr HA, Kirkpatrick CJ. Generation of human pulmonary microvascular endothelial cell lines. *Lab Invest*. 2001;81:1717-1727.
21. Creelan BC, Antonia S, Bepler G, Garrett TJ, Simon GR, Soliman HH. Indoleamine 2, 3-dioxigenase activity and clinical outcome following induction chemotherapy and concurrent chemo radiation in stage III non-small cell lung cancer. *Oncoimmunol*. 2013;2(3):e23438.
22. Visagie MH, Jaiswal SR, Joubert AM. In vitro assessment of a computer-designed potential anticancer agent in cervical cancer cells. *Biol Res*. 2016;49:43. doi:10.1186/s40569-016-0104-5
23. Feoktistova M, Geserick P, Leverkus M. Crystal Violet staining for determining viability of cultured cells. *Cold Spring Harb Protoc*. 2016;2016(4):87379. doi:10.1101/pdb.prot.087379
24. Walczak K, Żurawska M, Kiś J, et al. Kynurenic acid in human renal cell carcinoma: its antiproliferative and antimigrative action on Caki-2 cells. *Amino Acids*. 2012;43:1663-1670.
25. Walczak K, Deneka-Hannemann S, Jarosz B, et al. Kynurenic acid inhibits proliferation and migration of human glioblastoma T98G cells. *Pharmacol Rep*. 2014;66:130-136.
26. Walczak K, Langner E, Makuch-Kocka A, et al. Effect of tryptophan-derived AhR ligands, kynurenine, kynurenic acid and FICZ, on proliferation, cell cycle regulation and cell death of melanoma cells—in vitro studies. *Int J Mol Sci*. 2020;21:7946. doi:10.3390/ijms21217946
27. Conley-LaComb MK, Semaan L, Singareddy R, et al. Pharmacological targeting of CXCL12/CXCR4 signaling in prostate cancer bone metastasis. *Mol Cancer*. 2016;15(1). doi:10.1186/s12943-016-0552-0
28. Opitz CA, Litzenburger UM, Sahm F, et al. An endogenous tumour-promoting ligand of the human aryl hydrocarbon receptor. *Nature*. 2011;478(7368):197-203.
29. Al-Karagholi MAH, Hansen JM, Abou-Kassem D, et al. Phase 1 study to access safety, tolerability, pharmacokinetics and pharmaco-dynamics of kynurenine in healthy volunteers. *Pharmacol Res Perspect*. 2021;9(2):e00741. doi:10.1002/prp2.741
30. Thaker AI, Rao MS, Bishnupuri KS, et al. IDO1 metabolites activate β-catenin signaling to promote cancer cell proliferation and colon tumorigenesis in mice. *Gastroenterology*. 2013;145(2):416-425.e4.
31. Trott JF, Kim J, Aboud OA, et al. Inhibiting tryptophan metabolism enhances interferon therapy in kidney cancer. *Oncotarget*. 2016;7(41):66540-66557.
32. Buchanan JL, Rauckhorst AJ, Taylor EB. 3-Hydroxykynurenine is a ROS-inducing cytotoxic tryptophan metabolite that disrupts the TCA cycle. *BioRxiv*. 2023:548411. doi:10.1101/2023.07.10.548411
33. Johnson TI, Minteer CJ, Kottmann D, et al. Quantifying cell cycle-dependent drug sensitivities in cancer using a high throughput synchronisation and screening approach. *EBioMedicine*. 2021; 68:103396. doi:10.1016/j.ebiom.2021.103396
34. Song H, Park H, Kim YS, et al. L-kynurenine-induced apoptosis in human NK cells is mediated by reactive oxygen species. *Int Immunopharmacol*. 2011;11(8):932-938.
35. Mabeta P. Decreased secretion of vascular endothelial growth factor is associated with increased apoptosis in vascular tumor derived endothelial cells. *J Physiol Pharmacol*. 2013;64:473-477.
36. Zhai L, Bell A, Ladomersky E, et al. Immunosuppressive IDO in cancer: mechanisms of action, animal models and targeting strategies. *Front Immunol*. 2020;11:1185. doi:10.3389/fimmu.2020.01185
37. Girithar HN, Pires AS, Ahn SB, Guillemin GJ, Gluch L, Heng B. Involvement of the kynurenine pathway in breast cancer: updates on clinical research and trials. *BJC* 2023;129(2):185-203. doi:10.1038/s41416-023-02245-
38. Muller AJ, DuHadaway JB, Donover PS, Sutanto-Ward E, Prendergast GC. Inhi-bition of indoleamine 2,3-dioxygenase, an immunoregulatory target of thecancer suppression gene Bin1, potentiates cancer chemotherapy. *Nature Med*. 2005;11:312-319.
39. Munn DH, Shafizadeh E, Attwood JT, Bondarev I, Pashine A, Mellor AL. Inhibition of T cell proliferation by macrophage tryptophan catabolism. *J Exp Med*. 1999;189(9):1363-1372.
40. Heng B, Bilgin AA, Lovejoy DB, et al. Differential kynurenine pathway metabolism in highly metastatic aggressive breast cancer subtypes: beyond IDO1-induced immunosuppression. *Breast Cancer Res*. 2020;22(1):113. doi:10.1186/s13058-020-01351-1
41. Liu Q, Zhai J, Kong X, et al. Comprehensive analysis of the expression and prognosis for TDO2 in breast cancer. *Mol Ther Oncolyt*. 2020;17:153-168.
42. Chen IC, Lee KH, Hsu YH, Wang WR, Chen CM, Cheng YW. Expression pattern and clinicopathological relevance of the indoleamine 2,3-dioxygenase 1/tryptophan 2,3-dioxygenase protein in colorectal cancer. *Dis Markers*. 2016:8169724. doi:10.1155/2016/8169724
43. Zhao L, Wang B, Yang C, et al. TDO2 knockdown inhibits colorectal cancer progression via TDO2-KYNU-AhR pathway. *Gene*. 2021;792:145736.
44. Adams S, Teo C, McDonald KL, et al. Involvement of the kynurenine pathway in human glioma pathophysiology. *PLoS One*. 2014; 9(11):e112945.
45. Li L, Wang T, Li S, et al. TDO2 promotes the EMT of hepatocellular carcinoma through Kyn-AhR pathway. *Front Oncol. 2020*. 2020;10:562823. doi:10.3389/fonc.2020.562823
46. Pires AS, Sundaram G, Heng B, Krishnamurthy S, Brew BJ, Guillemin GJ. Recent advances in clinical trials targeting the kynurenine pathway. *J Pharm Thera*. 2021;236:108055. doi:10.1016/j.pharmathera.2021.1080550163-7258

SUPPORTING INFORMATION

Additional supporting information can be found online in the Supporting Information section at the end of this article.

How to cite this article: Nkandeu DS, Joubert AM, Serem JC, Bipath P, Hlophe YN. An exploratory study on the effect of kynurenine metabolites on sEnd-2 endothelioma cells. *Cell Biochem Funct*. 2024;42:e4065. doi:10.1002/cbf.4065